Analysis of foundations vibrating under harmonic loads during emergency shutdown due to additional pulse loading

Kirtika Samanta [a] and Priti Maheshwari [b,*]

[a] Research Scholar, Department of Civil Engineering, Indian Institute of Technology Roorkee, Roorkee-247667, India (Email: knavek2@gmail.com)

[b] Professor, Department of Civil Engineering, Indian Institute of Technology Roorkee, Roorkee-247667, India; Member, ISSMGE

(Email: priti_mahesh2001@yahoo.com; priti.maheshwari@ce.iitr.ac.in).

Mob: +91 9897888630, https://orcid.org/0000-0002-2979-8568/print

* Corresponding author

Abstract

This study uses an elastic-perfectly plastic single degree of freedom (SDOF) system to investigate reaction of machinery-supporting foundations to harmonic and pulse loads. An exponentially decaying pulse is used and applied to an already operating machine foundation which may experience an emergency shutdown due to extreme loading. Based on response at end of positive phase of pulse, two cases are analyzed. The governing equations are derived and solved numerically. Random response of SDOF system, before vibrations die out, can be observed due to the interaction of the two different loadings. Overestimation of the response for zero decay coefficient, *b* representing a triangular pulse, is noted. The absolute maximum displacement, influenced by the negative phase, changes by approximately 10-11% as the mass increases from 180 tons to 220 tons. Stiffness of the system and damping ratio affected the response to maximum extent. For various input parameters considered, displacement reduces by an order of 73% with increase in stiffness and by about 65% when damping ratio increased. The results indicate that negative phase of pulse loading has significant impact, particularly on less stiff and less damped systems.

Keywords: Machine foundation, harmonic loading, pulse loading, variable frequency, SDOF system, elastic-perfectly plastic (EPP) response, emergency shutdown.

1. Introduction

Many industrial machines require foundations that support reciprocating, impulsive, or rotary equipment. Foundations for these machines are exposed to dynamic loads beside static loads, where the dynamic loads acting due to the unbalanced forces, or inertia from the moving masses, arise during the operation of the machine. If not designed properly, the foundation-soil system experiences significant vibrations that can influence functioning of the machine and harm the people working nearby. Thus, designing these foundations aims to limit their amplitude within acceptable tolerances [1]. Throughout the years, various researchers have analyzed the response of machine foundations under the action of dynamic loadings [2-19].

An explosion due to mining, quarrying, or due to vibration transmission from another foundation supporting machinery in the vicinity [7, 20] may inflict significant loading in addition to the dynamic loads due to the operation of the machine. Apart from this, structures may also be subjected to seismic events where the response may be influenced by pulse-like ground motions [21-24]. Consequently, the foundation system may experience excessive vibrations, leading to an emergency shutdown of the machine. In addition, the behavior of the soil-foundation system will also change. Therefore, the dynamic response analysis to the interaction of harmonic and detonation (pulse like) loadings must be addressed for the efficacious design of these foundations.

An explosion rapidly releases energy, compressing the surrounding air and generating a forward-moving wave. This blast wave experiences a swift pressure increase that quickly drops to zero (compression or positive phase) and then falls below zero (suction or negative phase)

before returning to equilibrium. For simplification, various researchers have modeled it as a triangular pulse that decays linearly, neglecting its negative phase [25-30]. However, the actual behaviour is described using the nonlinear exponentially decaying function. Many researchers such as Li and Meng [31], Wei and Dharani [32], Teich and Gebbeken [33], Bryant et al. [34], Rigby et al. [35], Alisjahbana et al. [36], Maheshwari and Yadav [37], and Samanta and Maheshwari [38] emphasized on the importance of suction phase of pulse loading in the analysis of such systems.

Considering the extreme loading conditions during an explosion, the behaviour of the system cannot be regarded as elastic, and hence, over the years, several researchers have also investigated its elasto-plastic behaviour. Li and Meng [31] used rectangular, triangular, and exponential forms of pulse loading to analyse the response of an elastic-perfectly plastic (EPP) single degree of freedom (SDOF) structural system. Gantes and Pnevmatikos [39] studied the influence of the shape of the blast load-profile curve on the response of structures with the help of elastic-plastic response spectra. It was concluded that the triangular load-profile curve gives un-conservative results for flexible structures and over-conservative results for stiffer structural systems. Li et al. [26] computed an equivalent static force for an EPP-SDOF system to design RC frame structures subjected to blast loading. Rigby et al. [40] also employed similar system to obtain the response spectra for blast loads and used the linear acceleration explicit dynamics method to derive the dynamic equations of motion. Zheng et al. [41] used an elastic-plastic model to analyse stiffened plates subjected to blast loads. Most of these studies emphasize the effects of blast on the response analysis of structures or structural components. Few studies were conducted to investigate the impact of the blast loading on the dynamic response of elasto-plastic foundation systems [42-44]. Furthermore, fewer attempts have been made to investigate the analysis of how machine foundation systems respond elastically and plastically to blast loads [27, 38, 45, 46].

As previously mentioned, owing to the excessive vibration of the machine during an extreme loading condition, the machine may experience an emergency shutdown. Maheshwari and Naramsetti [27] and Samanta and Maheshwari [38] assumed that the machine would stop immediately if the system entered the plastic stage, which may be during or after the duration of blast loading. This may not be the case in reality. Whenever a machine experiences an emergency shutdown, it stops gradually with varying frequency [47]. Samanta and Maheshwari [45] attempted for such a situation, however, did not address the issue especially for EPP systems.

Keeping the above-stated points in mind, this study uses an elastic-perfectly plastic single degree of freedom (EPP-SDOF) system to analyse the response of an already operating machine foundation to the extreme loading condition. An exponentially decaying pulse capturing both the compressive (positive) and suction (negative) stages is used to idealize this loading. Upon entering the plastic region, it is expected that the machine will gradually come to a stop, with the exciting frequency exponentially decreasing until it eventually dissipates, thus addressing the gap in the existing literature. This study focuses on assessing the machine's behaviour during an emergency shutdown due to the extreme conditions of a blast. Two cases based on the positive phase duration, t_d are considered. Based on this, the governing dynamic equations are formulated and solved numerically with the help of fourth-order Runge-Kutta method. Subsequently, these solutions are used to compare pulse loading with varying extent of negative / suction phase and to emphasize its influence on the response of the machine-foundation system.

The analytical model for an EPP-SDOF system is formulated in the following section, along with the methodology for its solution in terms of displacement-time relationships. Emphasis is given to the influence of the varying extent of the suction stage of pulse during the emergency shutdown of the machine. A parametric study considering the effect of the mass of the machine

and foundation block, peak pulse magnitude, stiffness, frequency ratio, and damping ratio on the response of the SDOF system is conducted.

2. Modeling of Soil-Foundation System

A mass-spring-dashpot SDOF model is used to represent a machine foundation system vibrating in the vertical direction due to operation of machine. The governing dynamic equation of motion used to describe the SDOF system is given as,

$$m\ddot{x}(t) + c\dot{x}(t) + kx(t) = P \sin\omega t, \quad (1)$$

Here, m represents the mass of the machine and foundation block, c denotes the coefficient of viscous damping, and the equivalent spring constant k corresponds to the elastic resistance of the soil. P is the amplitude of the externally applied dynamic force originating from the machine's operating condition with ω as its exciting frequency. Displacement, velocity, and acceleration functions are given by $x(t)$, $\dot{x}(t)$, $\ddot{x}(t)$**,** respectively. It is assumed that the water table is situated below the level of the foundation, and the SDOF system is analysed for an underdamped case.

The analysis is conducted for a case where an explosion occurs at a significant distance from the foundation when the machine is under its operating conditions. There may be significant deformations without any physical damage to the system which will also depend upon the magnitude and distance of the blast from the target source. The pulse, idealizing the extreme loading, is applied directly to the foundation system, thus ignoring the effects due to propagation of waves as a consequence of the blast.

The blast load is modelled as a pulse having exponential decay function with a peak load F_o considering both the compression and suction stages. Both these stages are represented by the modified Friedlander's equation, as described by eq. (2) and shown in Fig. 1, which depends

on the time *t*, calculated from the onset of the pulse loading to the reference point [39, 48, 49, 50]. The equation is given as follows,

$$F(t) = F_o\left(1 - \frac{t}{t_d}\right)e^{-b\frac{t}{t_d}} \tag{2}$$

where t_d is the duration of the positive phase of pulse load, and *b*, the decay coefficient that determines the rate of decrease of load. The parameter *b* will always be greater than zero for a pulse with exponential decay function, where the extent of the suction stage depends on its specific values. $b = 0$ implies a particular case of triangular loading.

A bilinear resistance function representing the elastic-perfectly plastic SDOF system, as displayed in Fig. 2, comprises of four sections: (i) linear response with constant stiffness *k* till the elastic limit x_{el}, (ii) plastic response from the elastic limit x_{el} until the occurrence of maximum displacement x_m, characterized by a constant resistance R_m, (iii) unloading with the stiffness *k* till "resistance" $-R_m$ is reached, and (iv) plasticity in rebounding with a "resistance" $-R_m$, till the maximum displacement x_m' is obtained. These sections can be presented mathematically as follows,

$$R = \begin{cases} kx, & 0 < x < x_{el} \quad (section\,1) \\ R_m, & x_{el} < x < x_m \quad (section\,2) \\ R_m + k(x - x_m), & x_m - 2x_{el} < x < x_m \quad (section\,3) \\ -R_m, & x_m' < x < x_m - 2x_{el} \quad (section\,4) \end{cases} \tag{3}$$

These four sections form a full cycle, after which another cycle with four alike sections will commence and can be approached in a similar manner. Owing to the shape and short duration of the pulse loading, the maximum displacement of the SDOF system will primarily be obtained from the first cycle. Further, there will be no any change in the damping characteristics.

3. Analysis

The machine foundation system subjected to harmonic and pulse loading may behave elastically, wherein it experiences a jerk due to the pulse and starts vibrating in its operating condition [27]. However, for extreme loading conditions, the implementation of elastic-plastic analysis is more realistic. Also, excessive vibration of the machine during a blast may lead to an emergency shutdown. When the response of the foundation system enters the plastic region, an assumption is made that the machine will gradually stop operating with time with a frequency that varies exponentially.

The following equation gives the expressions for varying operating frequency of the machine with respect to time *t*,

$$\omega_1 = \omega e^{\frac{-t}{\tau}} \tag{4}$$

where ω is the initial value of the frequency at which the machine operates; τ is the time constant that influences the rate of decrease of operating frequency with time.

Eq. (4) suggests lower values of τ cause rapid decay of operating frequency to zero. The exponent in eq. (4) should always have a value less than zero to ensure that the system is stable and the frequency reduces with time. Having an exponent greater than zero causes the system to become unstable, as the frequency increases over time, which does not accurately represent an emergency shutdown condition.

3.1 *Cases considered for the study*

The dynamic analysis of the EPP-SDOF system is carried out and solutions for the governing equations of motion are derived. The system undergoes elastic vibration when subjected to a harmonic load from time $t = 0$. At time $t = t_1$, a pulse having positive phase duration, t_d (Fig. 1) is applied to the system. t_{el} represents the time at which the system enters the plastic domain. The corresponding displacements of the SDOF system are given by x_{t1}, x_{td}, and x_{el} respectively.

The system is assumed to experience an emergency shutdown when plasticity is mobilized. Further, it is also assumed that the maximum displacement x_m occurs after the time duration t_d [26, 27]. Two cases of analysis are considered based on relative values of x_{td} and x_{el} and are explained below,

i. Case 1: $x_{td} < x_{el}$ (Fig. 3(a)): Duration of compression stage of pulse (t_1 to t_d) gets over in elastic region, i.e., $t_{el} > t_d$. While the system is still in the elastic region, the pulse loading hits and the system then vibrates under its normal operating condition till the end of its elastic state represented by $t = t_{el}$. Subsequently, upon entering the plastic region, the machine experiences an emergency shutdown and its operating frequency disappears with time following an exponentially reducing function.

ii. Case 2: $x_{td} > x_{el}$ (Fig. 3(b)): The system undergoes a transition from the elastic to the plastic region during the compression stage of pulse, i.e., $t_1 < t_{el} < t_d$. Harmonic loading will still act upon the system on entering the plastic domain but with a varying operating frequency that will eventually disappear with time.

For the two cases, the governing equations of motion are similar; however, the initial conditions differ. These equations of motion are given as follows,

$$m\ddot{x}(t) + c\dot{x}(t) + kx(t) = P\sin\omega t, \qquad t \le t_1 \qquad (5a)$$

$$m\ddot{x}(t) + c\dot{x}(t) + kx(t) = P\sin\omega t + F_o\left(1 - \frac{t - t_1}{t_d}\right)e^{-b\left(\frac{t-t_1}{t_d}\right)}, \qquad t_1 \le t \le t_{el} \qquad (5b)$$

$$m\ddot{x}(t) + c\dot{x}(t) + R_m = P\sin\left(\omega e^{\frac{-(t-t_{el})}{\tau}} t\right) + F_o\left(1 - \frac{t - t_1}{t_d}\right)e^{-b\left(\frac{t-t_1}{t_d}\right)}, \qquad t_{el} \le t \le t_m \qquad (5c)$$

$$m\ddot{x}(t) + c\dot{x}(t) + \left[R_m + k\left(x - x_m\right)\right] = Psin(\omega e^{\frac{-(t-t_{el})}{\tau}} t) + F_o\left(1 - \frac{t - t_1}{t_d}\right) e^{-b\left(\frac{t-t_1}{t_d}\right)}, \quad t_m \le t \le t_{rb} \quad (5d)$$

$$m\ddot{x}(t) + c\dot{x}(t) - R_m = Psin(\omega e^{\frac{-(t-t_{el})}{\tau}} t) + F_o\left(1 - \frac{t - t_1}{t_d}\right) e^{-b\left(\frac{t-t_1}{t_d}\right)}, \quad t_{rb} \le t \le t_m' \quad (5e)$$

where, t_m corresponds to the time when displacement achieves a maxima x_m, as obtained in section 2 of Fig. 2. t_{rb} denotes the time at the end of the elastic rebounding stage where the corresponding displacement is $x = x_m - 2x_{el}$ (section 3 of Fig. 2). t_m' represents the time when displacement attains x_m' in section 4 (Fig. 2) due to the effect of the suction phase in exponential loading. The absolute maximum displacement of the system can be either of x_m or x_m', analogous to the first plastic stage and the plastic stage during rebound, respectively.

Following this, the system will behave in an elastic manner under the effect of decaying operating frequency of the machine, frequency of SDOF system, and initial conditions at the end of section 4 of Fig. 2.

The system might complete all four sections for the exponential loading, thus completing one cycle (Fig. 2). This will depend on the characteristics of the pulse (such as pulse shape, duration, and magnitude), all of which will be further exemplified in the upcoming sections.

Numerical differentiation techniques are employed to solve these dynamic equations of motion by applying the fourth-order Runge-Kutta method, which is widely used in solving the initial value problems for ordinary differential equations [51].

3.2 *Procedure for solving the dynamic equations of motion using the Runge-Kutta method*

The order of differential equation $\ddot{x}(t) = f(t, x, \dot{x}(t))$ is transformed from two to one by writing $\dot{x}(t) = z$ and the resulting equations are as given below,

$$\dot{x}(t) = z = f(t,x,z), \text{ and } \ddot{x}(t) = \dot{z} = \phi(t,x,z) \quad (6)$$

Conditions at time, t_o: $x(t_o) = x_o$, $z(t_o) = z_o$ (7)

Eq. (6) and conditions given by eq. (7) are employed to obtain the solutions for the equations corresponding to different chosen values of t.

In this study, initial conditions, i.e., the velocity and displacement at $t = 0$, are considered as zero for eq. (5a). For eqs. (5b-e), the velocity and displacement functions obtained at the end of previous time range, will be the primary conditions for the succeeding equation. $\dot{x}_{t1}$ and $x_{t1,}$ the velocity and displacement functions at time $t = t_1$ (from eq. 5a), are applied as the primary conditions for eq. (5b). Hence, the solution for the corresponding displacement x_1 and velocity $z_{1,}$ at time t_1 can be computed by the formula,

$$\begin{aligned} t_1 &= t_o + h \\ x_1 &= x_o + k \\ z_1 &= z_o + l \end{aligned} \quad \text{where} \quad \begin{cases} k = \frac{1}{6}(k_1 + 2k_2 + 2k_3 + k_4) \\ l = \frac{1}{6}(l_1 + 2l_2 + 2l_3 + l_4) \end{cases} \tag{8}$$

Using k_1, k_2, k_3, k_4 for $f(t, x, z)$ and l_1, l_2, l_3, l_4 for $\phi(t, x, z)$, Runge-Kutta expression develops into the following,

$$\begin{aligned} k_1 &= hf(t_o, x_o, z_o), & l_1 &= h\phi(t_o, x_o, z_o), \\ k_2 &= hf\left(t_o + \frac{1}{2}h, x_o + \frac{1}{2}k_1, z_o + \frac{1}{2}l_1\right), & l_2 &= h\phi\left(t_o + \frac{1}{2}h, x_o + \frac{1}{2}k_1, z_o + \frac{1}{2}l_1\right), \\ k_3 &= hf\left(t_o + \frac{1}{2}h, x_o + \frac{1}{2}k_2, z_o + \frac{1}{2}l_2\right), & l_3 &= h\phi\left(t_o + \frac{1}{2}h, x_o + \frac{1}{2}k_2, z_o + \frac{1}{2}l_2\right), \\ k_4 &= hf(t_o + h, x_o + k_3, z_o + l_3). & l_4 &= h\phi(t_o + h, x_o + k_3, z_o + l_3). \end{aligned}$$

Where t_o, x_o and z_o are the known initial conditions for the respective equation. The increment of the displacement x at each step is given by k, and the increment for velocity z is l, corresponding to the increment of the time t as h. A smaller step size h is chosen for more accurate results. To achieve the desired efficiency first, an interval h is chosen and the values of x and $\dot{x}$ are computed. Value of h is then halved and x and $\dot{x}$ are computed simultaneously. Then error E is estimated following eq. (9) and compared with a tolerance ε (=10^{-3}). For $E \leq \varepsilon$, the step size h is adopted which is halved for the case if $E \geq \varepsilon$.

$$E = \left| \frac{x_h(t) - x_{h/2}(t)}{x_h(t)} \right| \tag{9}$$

Accordingly, the step sizes are chosen between 0.0001 to 0.005 so that peaks of time-displacement history are captured properly. Replacement of t_o, x_o, z_o in eq. (8) with t_1, x_1, z_1 provides responses for the next time increment.

The solution for eq. (5a) is obtained by using the following equation and its initial conditions in the Runge Kutta expression eq. (8), for chosen values of the time t,

$$\begin{aligned} \dot{x}(t) &= z = f(t,x,z) \\ \ddot{x}(t) &= \dot{z} = \frac{P}{m}\sin\omega t - \frac{c}{m}z - \frac{k}{m}x = \phi(t,x,z) \end{aligned} \tag{10a}$$

Initial conditions: $x(0) = 0, z(0) = 0.$

Similarly, eq. (5b) is solved by employing the following equation and its initial condition,

$$\begin{aligned} \dot{x}(t) &= z = f(t,x,z) \\ \ddot{x}(t) &= \dot{z} = \frac{P}{m}\sin\omega t + \frac{F_o}{m}\left(1 - \frac{t - t_1}{t_d}\right)e^{-b\frac{t-t_1}{t_d}} - \frac{c}{m}z - \frac{k}{m}x = \phi(t,x,z) \end{aligned} \tag{10b}$$

Initial conditions: $x(t_1) = x_{t_1}, z(t_1) = \dot{x}_{t_1}$.

Consecutively for eq. (5c), the following equation and its initial condition are used,

$$\begin{aligned} \dot{x}(t) &= z = f(t,x,z) \\ \ddot{x}(t) &= \dot{z} = \frac{P}{m}\sin(\omega e^{\frac{-(t-t_{el})}{\tau}}t) + \frac{F_o}{m}\left(1 - \frac{t - t_1}{t_d}\right)e^{-b\frac{t-t_1}{t_d}} - \frac{c}{m}z - \frac{R_m}{m} = \phi(t,x,z) \end{aligned} \tag{10c}$$

Initial conditions: $x(t_{el}) = x_{el}, z(t_{el}) = \dot{x}_{tel}$.

Likewise, the following equation and its initial condition are employed for eq. (5d),

$$\begin{aligned} \dot{x}(t) &= z = f(t,x,z) \\ \ddot{x}(t) &= \dot{z} = \frac{P}{m}\sin(\omega e^{\frac{-(t-t_{el})}{\tau}}t) + \frac{F_o}{m}\left(1 - \frac{t - t_1}{t_d}\right)e^{-b\frac{t-t_1}{t_d}} + \frac{kx_m - R_m}{m} - \frac{c}{m}z - \frac{k}{m}x = \phi(t,x,z) \end{aligned} \tag{10d}$$

Initial conditions: $x(t_m) = x_m, z(t_m) = 0.$

For eq. (5e), the following equation and its initial condition are used,

$$\dot{x}(t) = z = f(t,x,z)$$

$$\ddot{x}(t) = \dot{z} = \frac{P}{m} sin(\omega e^{\frac{-(t-t_{el})}{\tau} t}) + \frac{F_o}{m}\left(1 - \frac{t - t_1}{t_d}\right) e^{-b\frac{t-t_1}{t_d}} - \frac{c}{m} z + \frac{R_m}{m} = \phi(t,x,z) \quad (10e)$$

Initial conditions: $x(t_{rb}) = x_m - 2x_{el}, z(t_{rb}) = \dot{x}_{t_{rb}}$.

The methodology is confirmed using studies from the existing literature and presented in the subsequent section. Thereafter, time-displacement histories are acquired for the cases mentioned above to investigate the response of the SDOF system.

4. Validation of the Study

The response of the SDOF system to the exponentially varying pulse loading is validated by the Gantes and Pnevmatikos [39] as shown in Fig. 4. Gantes and Pnevmatikos [39] analyzed an elastic-perfectly plastic SDOF system for a time period T = 1 s. They used blast arrival time as zero and the response was reported as x/x_{el} with t_d = 0.2 s. The harmonic loading is considered as zero for the present work, and other input parameters from Gantes and Pnevmatikos [39] are used. The maximum response is obtained as x/x_{el} = 1.37, identical to that documented by Gantes and Pnevmatikos [39].

Further, an attempt is also made to compare the findings of present study with experimental results available in the literature. To address this, reference is made to an experimental study conducted by Surapreddi and Ghosh [13]. For comparison a special case of present work, in the absence of pulse loading, is considered. Results exhibit strong concordance near the resonance. For eccentric force setting of 0.090, 0.134, 0.172 N-sec^2, the amplitudes of vertical displacement are found to be 0.563, 0.707, and 0.861 mm from the present study as against 0.566, 0.706, and 0.860 mm from Surapreddi and Ghosh [13], respectively.

5. Results and Discussion

The governing equations of motion for the two cases are simulated to obtain displacement-time graphs for various parameters to analyze the response of the SDOF system to complex loading as discussed above. The study incorporates input parameters sourced from existing literature, detailed in Table 1. A positive phase duration of 0.005 s and 0.01 s are chosen for Case 1 and Case 2, respectively [8, 35]. The SDOF system's response is comparable in both cases, albeit with higher displacement magnitudes observed in Case 2. This phenomenon is attributed to the system transitioning from the elastic to plastic region during the pulse, coupled with a longer duration of the positive phase in Case 2. The possibility of resonance is not considered in this study. The results obtained are presented in this section by means of displacement-time plots.

5.1 *Influence of time constant, τ*

The influence of τ for b equal to unity for Case 1 and Case 2 is depicted in Figs. 5 and 6, respectively. The machine operates in elastic domain under the influence of only harmonic loading till 3 s. The response shoots up due to the application of the pulse and the system enters the plastic stage. Concurrently, there is a gradual decline in the operational frequency, which diminishes over time based on the specified time constant. The system enters the plasticity region twice, thus completing an entire cycle (Fig. 2), and then performs with varying operational frequency of the machine which eventually dies out.

Appropriate values of τ are adopted from speed vs. time curves after shutdown as provided by Kurz et al. [47] for various types of machines. As the value of the time constant increases, the machine operates for a longer time with an exponentially decreasing frequency before finally coming to a halt. In other words, higher the value of τ, longer the machine will vibrate before it ceases to operate. The machine will vibrate for about 200 s, 800 s, and 1800 s for τ values of 10 s, 40 s, and 100 s, respectively before ultimately coming to a stop, for the set of input

parameters given in Figs. 5 and 6. The response gets random during the rebounding after the second plastic stage between the time instance between 3.5 to 5 s. This randomness in the response is attributed to the interaction of the pulse and harmonic loads with varying exciting frequency.

5.2 *Influence of the decay coefficient, b*

Decay coefficient, b is a non-dimensional parameter influencing the shape of pulse and the magnitude of the suction phase, as depicted in Fig. 1. Greater extent of the suction/negative phase signifies that $b < 1$. In this study, various values of b ranging from 0 to 3 are selected. Specifically, $b = 0$ corresponds to a triangular profile, $b = 0.8$ represents a load profile with a more pronounced suction phase, $b = 1$ reflects a load profile validated experimentally by Jacinto et al. [52], and $b = 2$ and $b = 3$ are included for comparative purposes. The results are presented for both cases of analysis in Fig. 7. The maximum response for the triangular distribution of pulse loading is much higher than the exponential loading because of the faster decay of the exponential distribution of pulse loading than the triangular one.

The system with values of $b = 0.8$ and 1 undergoes elastic behaviour followed by plastic behaviour where the first peak response x_m is obtained. Subsequently, the system rebounds and attains the second peak response x_m', completing one entire cycle (Fig. 2). The system then vibrates elastically with random vibration which dies out with time.

The second peak displacement may take either negative or positive values as per properties of the pulse. It is evident from Fig. 7 that the second peak displacement is more pronounced than the first peak displacement when compared in its absolute values for b less than unity. This is ascribed to the impact of the suction phase during elastic rebounding. Similar behavior is also observed with reference to response of various structural components as presented by Wei and Dharani [32] and Aune et al. [53].

For $b = 2$ and $b = 3$, the system reaches its first peak x_m immediately following the compressive phase t_d of the pulse and subsequently undergoes elastic motion without transitioning back into the plastic deformation stage. This behavior may be due to the diminishing influence of the suction phase for values of $b > 1$. Likewise, in the absence of a negative phase for $b = 0$, the system obtains its maximum displacement after the positive phase duration and does not enter the plasticity stage again. The table presents the maxima of displacement magnitude for various values of b (decay coefficient), as detailed in Table 2.

Fig. 7 and Table 2 suggest that the response is significantly overestimated in case of a triangular pulse ($b = 0$). The exponentially decaying pulse, taking into account both the positive and negative phases, provides a more realistic way of modeling the extreme loading conditions.

Subsequently, the impact of the suction phase on the response of the SDOF system is examined through a parametric analysis. The effect of different parameters is evaluated by calculating the displacement response using the dynamic equations of motion provided and presenting the time-displacement graphs (Figs. 8-12). Various parameters include mass of the machine and foundation block, peak pulse magnitude, stiffness, frequency ratio, and damping ratio. The value of the decay coefficient is chosen as 0.8 throughout the parametric study to illustrate the impact of the suction phase of the pulse. The modulus of maximum displacement of the SDOF system could be any of two peak displacements, viz., x_m corresponding to the compressive phase of pulse and x_m' due to the suction stage of the pulse. Results from the parametric study are quantified, expressed in terms of the absolute maximum displacement, and presented in subsequent sections.

5.3 *Influence of mass of the machine and foundation block, m*

Fig. 8 depicts effect of parameter, m on the response of SDOF system. As the mass varies, a phase difference in the response is noted during the elastic vibration stage. The system's

response is higher for Case 2 compared to Case 1 owing to its transition from elastic to plastic state during the pulse and also due to the longer compressive pulse for Case 2. On account of increase in the inertial force with increase in mass, the maximum displacements (both x_m and x_m') decrease for Case 2 (Fig. 8b). However, for Case 1, the first peak x_m decreases with the increase in mass, and the second peak x_m' increases with increase in mass, due to the combination of negative pulse and elastic rebounding (Fig. 8a). For better clarity, absolute values of peak displacement are presented in Table 3 and it can be observed that the absolute values of x_m' are significantly higher than those of x_m, highlighting the impact of the suction stage of the pulse. The modulus of x_m' resulted from the impact of the suction phase, increases by 11% for Case 1, and decreases by 10% for Case 2 with as parameter, m changes from 180 t to 220 t.

5.4 *Impact of peak pulse load magnitude, F_o*

The maximum displacement of the system shows an increasing trend with the rise in parameter, F_o, as shown in Fig. 9. The results are also presented in Table 4 in terms of peak displacements. The displacement x_m', occurring in the second plastic stage, is significantly higher than x_m, which occurs in the first plastic stage. x_m' increases by about 43% and 24%, respectively, for Case 1 and Case 2 with the increase in peak magnitude of pulse, F_o from 900 kN to 1100 kN.

5.5 *Influence of stiffness, k*

The impact of stiffness on displacements is presented in Fig. 10 and maximum displacements are shown in Table 5. Displacements are bound to be higher for systems with low stiffness. Modulus value of displacement is reported to be reducing by approximately 64% and 73% respectively, for Cases 1 and 2, with an escalation in stiffness value from 100 kN/mm to 810 kN/mm. Effect of the negative phase of pulse loading on the maximum response is more

prominent for low stiffness values, i.e., for relatively flexible systems. For Case 2, the absolute difference in the two peak displacements is found to be 2.416 mm, 1.733 mm, and 0.847 mm for stiffness values of 100 kN/mm, 200 kN/mm, and 810 kN/mm, respectively.

5.6 *Influence of frequency ratio, f_r*

The frequency ratio is varied from 0.5 to 1.6, and respective results are depicted in Fig. 11. With the increase in f_r from 0.5 to 0.7, the maximum responses of the system, x_m and x_m' increase marginally by about 4% (Case 1) and 3% (Case 2). However, with additional increase in the value of f_r from 0.7 to 1.6, the maximum displacements are found to reduce by about 6% and 8% respectively, for Cases 1 and 2. There is minimal impact observed on the peak response with variations in frequency ratio, as indicated in Table 6. This is due to the reason that maximum response is obtained after the system transitions into the plastic domain where the exciting frequency gradually reduces.

5.7 *Influence of damping, ζ*

The damping ratio ranges from 0 to 25% and its impact on the response is presented in Fig. 12. On increasing ζ from 0 to 25%, a corresponding reduction of 54% (Case-1) and 66% (Case-2) in the absolute maximum displacement is observed. The time of occurrence of peak response also reduces for more damped system. Table 7 indicates that the effect of suction stage of pulse in terms of the second peak displacement is more predominant for the undamped system and systems with lower damping ratio values. The randomness in response of the system in rebounding stage due to the interaction of two loadings is not observed for the undamped system, which undergoes sinusoidal oscillations.

The result of this study is presented under the combined influence of harmonic and pulse loading. This information can be utilized to design effective vibration mitigation measures [54],

particularly in scenarios where such loading conditions are expected, ensuring optimal performance of the foundation. The following section discusses the key conclusions drawn from this study.

6. Conclusions

Dynamic response analysis of a soil-machine foundation system was studied in the event of an emergency shutdown of the machine due to extreme loading from a blast. It was assumed that machine on entering the plastic stage, will continue to oscillate but with a decreasing frequency which will eventually disappear with time. Due to the interaction of the two different loadings, a random response of the SDOF system was observed in the rebounding stage before the vibration dies out and the machine ceases to operate. The impact of various system parameters on the response of the SDOF system was summarized in terms of the absolute maximum displacement (either of x_m and x_m'). The following conclusions were drawn from the detailed study conducted in this paper:

i) A notable impact of the suction phase of pulse loading on the maximum response was observed by varying the decay coefficient of pulse, b. For values of b less than unity, the absolute value of x_m' was more pronounced than x_m. This was due to the combined effect of negative phase and elastic effects of rebounding stage.

ii) Any variation in mass has a significant impact on the response of the SDOF system. The maximum displacement due to the influence of the negative phase increases by 11% for Case 1 and decreases by 10% for Case 2 as there is a rise in mass from 180 t to 220 t. In addition, a phase difference was observed in the response of the SDOF system while the system is in the elastic region for both cases.

iii) Peak pulse load affects the response considerably as very high displacement was observed on increasing the pulse load magnitude. The absolute maximum displacement was found to

increase by about 43% and 24% respectively when the peak pulse magnitude was increased from 900 kN to 1100 kN.

iv) Both cases of analysis exhibited a reduction in the absolute maximum displacement when the stiffness is varied from 100 kN/mm to 810 kN/mm. The pronounced second peak displacement was observed specifically for flexible systems.

v) The frequency ratio has a minor impact on the system's response in elastic-plastic cases, primarily due to the gradual decrease in the operational frequency during the plastic stage.

vi) An increase in damping ratio from 0 to 25% was found to decrease the system's response by 54% and 66%, respectively for both cases, and was also found to reduce the time for peak displacement. Additionally, the influence of the suction phase was observed to be more dominant for undamped systems and systems with lower values of damping ratio.

Several aspects, such as modeling wave propagation from blasts, changes in damping conditions during transition from elastic to EPP response, and the shape of pulse loading, are of significant importance and represent future endeavors for the authors. Results presented in this study can help in designing the machine foundations for emergency shutdown conditions where such type of loading is expected. Further, presented approach and the derived information can help in designing suitable vibration barrier systems for such a soil-foundation system.

References

1. Gazetas G. “Analysis of machine foundation vibrations: state of the art”, *Soil Dynamics and Earthquake Engineering*, 2(1), pp. 2-42 (1983), 10.1016/0261-7277(83)90025-6.

2. Sankaran K.S. and Subrahmanyam M.S. “Prediction of vertical vibrations of footings by mass-spring-dashpot model”, *Soils and Foundations*, 17(1), pp. 53-64 (1977), 10.3208/sandf1972.17.53.

3. El Hifnawy L. and Novak M. “Response of hammer foundations to pulse loading”, *Soil Dynamics and Earthquake Engineering*, 3(3), pp. 124–132 (1984), 10.1016/0261-7277(84)90042-1.

4. Nayfeh A. H. and Serhan S. J. “Vertical vibration of machine foundation” *Journal of Geotechnical Engineering, ASCE*, 115(1), pp. 56-74 (1989), 10.1061/(ASCE)0733-9410(1989)115:1(56).

5. Sridharan A., Baidya D. K. and Raju D. M. “Analog solutions for design of machine foundations”, *Soils and Foundations*, 30(4), pp. 53-62 (1990), 10.3208/sandf1972.30.4_53.

6. Aşik M. Z. “Dynamic response analysis of the machine foundations on a homogeneous soil layer”, *Computers and Geotechnics*, 24(2), pp. 141–153 (1999), 10.1016/s0266-352x(98)00032-9.

7. El Naggar M. H. “Evaluation of performance of machine foundation under blast-induced excitation”, In Structures under Shock and Impact VI, eds. N. Jones and C. A. Brebbia, pp. 47-56, WIT Press, UK (2000), 10.2495/SU000041.

8. Chehab A. G. and El Naggar M. H. “Response of block foundations to impact loads”, *Journal of Sound and Vibration*, 276(1-2), pp. 293–310 (2004), 10.1016/j.jsv.2003.07.028.

9. Chen S. S. and Shi J. Y. “Simplified model for vertical vibrations of surface foundations”, *Journal of Geotechnical and Geoenvironmental Engineering, ASCE*, 132(5), pp. 651-655 (2006), 10.1061/(ASCE)1090-0241(2006)132:5(651).

10. Senjuntichai T., Keawsawasvong S. and Plangmal R. “Vertical vibrations of rigid foundations of arbitrary shape in a multi-layered poroelastic medium”, *Computers and Geotechnics*, 100, pp. 121-134 (2018), 10.1016/j.compgeo.2018.04.012.

11. Trąbka A. “Effect of pulse shape and duration on dynamic response of a forging system”, *Acta Mechanica et Automatica*, 13(4), pp. 226-232 (2019), 10.2478/ama-2019-0030.

12. Senjuntichai T., Keawsawasvong S. and Rajapakse R. K. N. D. “Vertical vibration of a circular foundation in a transversely isotropic poroelastic soil”, *Computers and Geotechnics*, 122, Article 103550 (2020), 10.1016/j.compgeo.2020.103550.

13. Surapreddi S. and Ghosh P. “Experimental and numerical investigations on attenuation response of machine foundations under vertical excitation”, *Geomechanics and Geoengineering*, 17(6), pp. 1865-1886 (2021), 10.1080/17486025.2021.1980231.

14. Giorgetti S., Giorgetti A., Jahromi R. T. et al. “Machinery foundations dynamical analysis: a case study on reciprocating compressor foundation”, *Machines*, 9, 228 (2021), 10.3390/machines9100228.

15. Rajkumar K., Ayothiraman R. and Matsagar V. A. “Effects of soil-structure interaction on torsionally coupled base isolated machine foundation under earthquake load”, *Shock and Vibration*, 2021, 6686646 (2021), 10.1155/2021/6686646.

16. Abdulrasool A. S., Fattah M. Y. and Salim, N. M. “Displacements and stresses induced by vibrations of machine foundation on clay soil of different degrees of saturation”, *Case Studies in Construction Materials*, 17, e01327 (2022), 10.1016/j.cscm.2022.e01327.

17. Rizvi S. M. H., Wang K., Jala F. E. et al. “Evaluation of capacity of power hammer machine foundation from high strain dynamic load test: field test and axisymmetric numerical modelling”, *Transportation Geotechnics*, 36, 100826 (2022), 10.1016/j.trgeo.2022.100826.

18. Amiri A., Tafreshi S. N. M., Dawson A. R. et al. “Machine foundation response subjected to vertical vibration: experimental and analytical using cone model”, *European Journal of*

Environmental and Civil Engineering, 27(13), pp. 3920-3950 (2023), 10.1080/19648189.2023.2165164.

19. Shi J.-Y., Chen S.-S. and Chen K.-Y. "A simplified model of layered soil for analysing vertical vibration of loaded foundations", *Structure and Infrastructure Engineering*, 19 (1), pp. 21-38 (2023), 10.1080/15732479.2021.1919152.

20. El Naggar M. H. "Performance evaluation of vibration-sensitive equipment foundations under ground-transmitted excitation", *Canadian Geotechnical Journal*, 40(3), pp. 598-615 (2003), 10.1139/t03-014.

21. Yaghmaei-Sabegh S. "Evaluation of pulse effect on frequency content of ground motions and definition of a new characteristic period", *Earthquakes and Structures*, 20(4), pp. 457-471 (2021), 10.12989/eas.2021.20.4.457.

22. Repapis C. C., Mimoglou P. P., Dimakopoulou V. V., et al. "Efficient strong motion duration of pulse-like records for nonlinear structural analyses", *Earthquake Engineering and Structural Dynamics*, 49, pp. 479-497 (2020), 10.1002/eqe.3249.

23. Yaghmaei-Sabegh S., Jafari-Koucheh E. and Ebrahimi-Aghabagher, M. "Estimating the seismic response of nonlinear structures equipped with nonlinear viscous damper subjected to pulse-like ground records", *Structures*, 28, pp. 1915-1923, (2020), 10.1016/j.istruc.2020.10.011.

24. Gan L.-L. and She G.-L. "Nonlinear transient response of magneto-electro-elastic cylindrical shells with initial geometric imperfection", *Applied Mathematical Modelling*, 132 pp. 166-186 (2024), 10.1016/j.apm.2024.04.049.

25. Krauthammer T. and Altenberg A. "Negative phase blast effects on glass panels", *International Journal of Impact Engineering*, 24(1), pp. 1–17 (2000), 10.1016/S0734-743X(99)00043-3.

26. Li B., Rong H.-C. and Pan T.-C. “Drift-controlled design of reinforced concrete frame structures under distant blast conditions- part I: theoretical basis”, *International Journal of Impact Engineering*, 34(4), pp. 743-754 (2007), 10.1016/j.ijimpeng.2006.01.010.

27. Maheshwari P. and Naramsetti B. S. “Closed form solutions for response of machine foundations under accidental blast loads”. *Soil Dynamics and Earthquake Engineering*, 116, pp. 386-396 (2019), 10.1016/j.soildyn.2018.10.016.

28. Hadianfard M. A. and Shekari M. “An equivalent single-degree-of-freedom system to estimate nonlinear response of semi-fixed flexural members under impact load”, *Iranian Journal of Science and Technology, Transactions of Civil Engineering*, 43 (supplement issue 1), pp. 343–355 (2019), 10.1007/s40996-018-0169-1.

29. Caçoilo A., Mourão R., Teixeira-Dias F. et al. “Structural response of corrugated plates under blast loading: the influence of the pressure-time history”, *Structures*, 30, pp. 531-545 (2021), 10.1016/j.istruc.2021.01.025.

30. Samanta K. and Maheshwari P., “Influence of harmonic and pulse excitations on response of foundations”, *International Journal of Geotechnical Engineering*, 17(1), pp. 40-59 (2023a), 10.1080/19386362.2022.2154921.

31. Li Q. M. and Meng H. “Pulse loading shape effects on pressure–impulse diagram of an elastic-plastic, single-degree-of-freedom structural model”, *International Journal of Mechanical Sciences*, 44(9), pp. 1985–1998 (2002), 10.1016/S0020-7403(02)00046-2.

32. Wei J. and Dharani L. R. “Response of laminated architectural glazing subjected to blast loading”, *International Journal of Impact Engineering*, 32, pp. 2032–2047 (2006), 10.1016/j.ijimpeng.2005.05.012.

33. Teich M. and Gebbeken N. “The influence of the underpressure phase on the dynamic response of structures subjected to blast loads”, *International Journal of Protective Structures*, 1(2), pp. 219-234 (2010), 10.1260/2041-4196.1.2.219.

34. Bryant L. M., Erekson J. M. and Herle K. W. “Are you positive about negative phase?” *Proceedings of Structures Congress 2013, ASCE,* Pittsburgh, Pennsylvania, USA, pp. 103–114, 10.1061/9780784412848.010.

35. Rigby S. E., Tyas A., Bennett T. et al. “The negative phase of the blast load”, *International Journal of Protective Structures*, 5(1), pp. 1–20 (2014a), 10.1260/2041-4196.5.1.1.

36. Alisjahbana S. W., Safrilah S., Putra J. C. P. et al. “Dynamic response of pavement plates to the positive and negative phases of the Friedlander load”, *Strength of Materials*, 50(2), pp. 702-710 (2018), 10.1007/s11223-018-0015-5.

37. Maheshwari P. and Yadav S. K. “Vibration analysis of foundations subjected to pulse excitations with negative phase”, *Indian Geotechnical Journal*, 52(5), pp. 1065-1078 (2022), 10.1007/s40098-021-00589-6.

38. Samanta K. and Maheshwari P. “Effect of negative phase of pulse loading on response of machine foundations vibrating under harmonic loads” *Mechanics Based Design of Structures and Machines*, 51 (11), pp. 6008-6022 (2023b), 10.1080/15397734.2022.2027782.

39. Gantes C. J. and Pnevmatikos N. G. “Elastic-plastic response spectra for exponential blast loading”, *International Journal of Impact Engineering*, 30(3), pp. 323–343 (2004), 10.1016/S0734-743X(03)00077-0.

40. Rigby S. E., Tyas A. and Bennett T. “Elastic-plastic response of plates subjected to cleared blast loads”, *International Journal of Impact Engineering*, 66, pp. 37-47 (2014b), 10.1016/j.ijimpeng.2013.12.006.

41. Zheng C., Kong X-s., Wu W-g. et al. “The elastic-plastic dynamic response of stiffened plates under confined blast load”, *International Journal of Impact Engineering*, 95, pp. 141-153 (2016), 10.1016/j.ijimpeng.2016.05.008.

42. Souli M. and Shahrour I. “Arbitrary Lagrangian Eulerian formulation for soil structure interaction problems”, *Soil Dynamics and Earthquake Engineering*, 35, pp. 72-79 (2012), 10.1016/j.soildyn.2011.10.006.

43. Jayasinghe L. B., Thambiratnam D. P., Perera N. et al. “Blast response and failure analysis of pile foundations subjected to surface explosion”, *Engineering Failure Analysis*, 39, pp. 41-54 (2014), 10.1016/j.engfailanal.2014.01.013.

44. Jayasinghe L. B., Zhao Z. Y., Goh A. T. C. et al. “A field study on pile response to blast-induced ground motion”, *Soil Dynamics and Earthquake Engineering*, 114, pp. 568-575 (2018), 10.1016/j.soildyn.2018.08.008.

45. Samanta K. and Maheshwari P. “Elasto-plastic analysis of foundations during emergency shutdown due to blast loading”, *International Journal of Protective Structures*, 15(2), pp. 359-386 (2024 a), 10.1177/20414196231174916.

46. Samanta K. and Maheshwari P. “Elasto-plastic analysis of machine foundations under harmonic and pulse loading with negative phase”, *Indian Geotechnical Journal*, (2024 b), 10.1007/s40098-024-00939-0.

47. Kurz R., Mendoza R., Burnes D. et al. “On gas turbine safety in offshore applications”, *Proc. ASME Turbo Expo 2018: Turbomachinery Technical Conference and Exposition*, Volume 9: Oil and Gas Applications; Supercritical CO2 Power Cycles; Wind Energy, Oslo, Norway, V009T27A002 (2018), 10.1115/GT2018-75003.

48. Karlos V., Larcher M. and Solomos G. “Analysis of the blast wave decay coefficient in the Friedlander equation using the Kingery-Bulmash data”, *Technical Report JRC94784*, Joint Research Centre, Ispra, Italy (2015).

49. Yuan Y., Zhu L., Bai X. et al. “Pressure–impulse diagrams for elastoplastic beams subjected to pulse-pressure loading”, *International Journal of Solids and Structures*, 160, pp. 148-157 (2019), 10.1016/j.ijsolstr.2018.10.021.

50. Yang T., Luo Y., Hu G. et al. “Probability distribution and determination of blast loading during structural blast resistant study”. *Shock and Vibration*, Article 7367288 (2022), 10.1016/j.istruc.2020.10.011.

51. Islam M. A. “Accurate solutions of initial value problems for ordinary differential equations with the fourth order Runge Kutta method”, *Journal of Mathematics Research*, 7(3), pp. 41-45 (2015), 10.5539/jmr.v7n3p41.

52. Jacinto A. C., Ambrosini R. D. and Danesi R. F. “Experimental and computational analysis of plates under air blast loading”, *International Journal of Impact Engineering*, 25(10), pp. 927–947 (2001), 10.1016/S0734-743X(01)00031-8.

53. Aune V., Valsamos G., Casadei F. et al. “Numerical study on the structural response of blast-loaded thin aluminium and steel plates”, *International Journal of Impact Engineering*, 99, pp. 131-144 (2017), 10.1016/j.ijimpeng.2016.08.010.

54. Jayawardana P., Thambiratnam D. P., Perera N. et al. “Use of artificial neural network to evaluate the vibration mitigation performance of geofoam-filled trenches”, *Soils and Foundations*, 59, pp. 874-887 (2019), 10.1016/j.sandf.2019.03.004.

55. Vucetic M. and Dobry R. “Effect of soil plasticity on cyclic response”, *Journal of Geotechnical Engineering, ASCE*, 117(1), pp. 89–107 (1991), 10.1061/(ASCE)0733-9410(1991)117:1(89).

56. IS: 2974 (Part I) “Code of practice for design and construction of machine foundations: part 1 foundation for reciprocating type machines”, New Delhi: Bureau of Indian Standards, (2008).

57. Selvadurai A. P. S. “Elastic Analysis of Soil-Foundation Interaction”, Elsevier Scientific Publishing Company, The Netherlands, (1979).

TABLE CAPTIONS

Table 1. Range of values for different parameters.

Table 2. Maximum response of the SDOF system for different values of decay coefficient.

Table 3. Maximum response of the SDOF system on varying the mass of machine and foundation block.

Table 4. Maximum response on varying the peak pulse load magnitude.

Table 5. Maximum response: variation in stiffness.

Table 6. Maximum response on varying frequency ratio.

Table 7. Maximum response on varying the damping ratio.

FIGURE CAPTIONS

Fig. 1. Pulse loading variation with time for decay coefficients.

Fig. 2. Resistance-displacement relationship of an EPP-SDOF system.

Fig. 3. Two cases of analysis

Fig. 4. Validation with work of Gantes and Pnevmatikos (2004).

Fig. 5. Response of the SDOF system to the various time constant values: Case 1.

Fig. 6. Response of the SDOF system to the various time constant values: Case 2.

Fig. 7. Influence of decay coefficient on the response of the SDOF system.

Fig. 8. Response of the SDOF system for variation in mass.

Fig. 9. Response of the SDOF system for variation in peak pulse magnitude.

Fig. 10. Response of the SDOF system for different values of stiffness.

Fig. 11. Response of the SDOF system for different values of the frequency ratio.

Fig. 12. Response of the SDOF system for different values of damping ratios.

Table 1. Range of values for different parameters.

Parameter	Range of Values
Mass of machine and foundation block (m)	220-180 tonnes [8]
Peak pulse load magnitude (F_o)	1100-900 kN [27]
Damping ratio (ζ)	25-0 % [55]
Stiffness (k)	810-100 kN/mm [8]
Frequency ratio (f_r)	1.6-0.5 [56]
Maximum resistance (R_m)	40 kN [57]
Decay coefficient (b)	3-0 [33, 39]
Time constant (τ)	100-10 s [47]

Table 2. Maximum response of the SDOF system for different values of decay coefficient.

Decay coefficient, *b*	**Maximum Displacement (mm)**			
	Case 1		Case 2	
	First peak x_m as obtained from the first plastic stage	Second peak x_m' after the rebounding stage	First peak x_m as obtained from the first plastic stage	Second peak x_m' after the rebounding stage
0	0.337	-	1.054	-
0.8	0.082	-0.236	0.291	-0.556
1	0.086	-0.029	0.300	0.091
2	0.115	-	0.354	-
3	0.094	-	0.278	-

Table 3. Maximum response of the SDOF system on varying the mass of machine and foundation block.

Mass of machine and foundation block, *m* (t)	**Maximum Displacement (mm)**			
	Case 1		Case 2	
	First peak x_m as obtained from the first plastic stage	Second peak x_m' after the rebounding stage	First peak x_m as obtained from the first plastic stage	Second peak x_m' after the rebounding stage
180	0.088	-0.223	0.319	-0.583
200	0.082	-0.236	0.291	-0.556
220	0.072	-0.248	0.260	-0.527

Table 4. Maximum response on varying the peak pulse load magnitude.

Peak magnitude of pulse load, F_o (kN)	**Maximum Displacement (mm)**			
	Case 1		Case 2	
	First peak x_m as obtained from the first plastic stage	Second peak x_m' after the rebounding stage	First peak x_m as obtained from the first plastic stage	Second peak x_m' after the rebounding stage
900	0.074	-0.188	0.258	-0.494
1000	0.082	-0.236	0.291	-0.556
1100	0.09	-0.268	0.325	-0.611

Table 5. Maximum response: variation in stiffness.

Stiffness, *k* (kN/mm)	**Maximum Displacement (mm)**			
	Case 1		Case 2	
	First peak x_m as obtained from the first plastic stage	Second peak x_m' after the rebounding stage	First peak x_m as obtained from the first plastic stage	Second peak x_m' after the rebounding stage
100	0.108	-0.661	0.370	-2.046
200	0.085	-0.531	0.332	-1.401
810	0.082	-0.236	0.291	-0.556

Table 6. Maximum response on varying frequency ratio.

Frequency ratio, f_r	**Maximum Displacement (mm)**			
	Case 1		Case 2	
	First peak x_m as obtained from the first plastic stage	Second peak $x_m{}'$ after the rebounding stage	First peak x_m as obtained from the first plastic stage	Second peak $x_m{}'$ after the rebounding stage
0.5	0.082	-0.236	0.291	-0.556
0.7	0.083	-0.246	0.292	-0.573
1.6	0.078	-0.231	0.284	-0.530

Table 7. Maximum response on varying the damping ratio.

Damping ratio, ζ (%)	**Maximum Displacement (mm)**			
	Case 1		Case 2	
	First peak x_m as obtained from the first plastic stage	Second peak x_m' after the rebounding stage	First peak x_m as obtained from the first plastic stage	Second peak x_m' after the rebounding stage
0	0.087	-0.268	0.322	-0.739
5	0.082	-0.236	0.291	-0.556
10	0.079	-0.185	0.267	-0.419
15	0.075	-0.174	0.247	-0.340
20	0.072	-0.144	0.230	-0.288
25	0.069	-0.122	0.215	-0.252

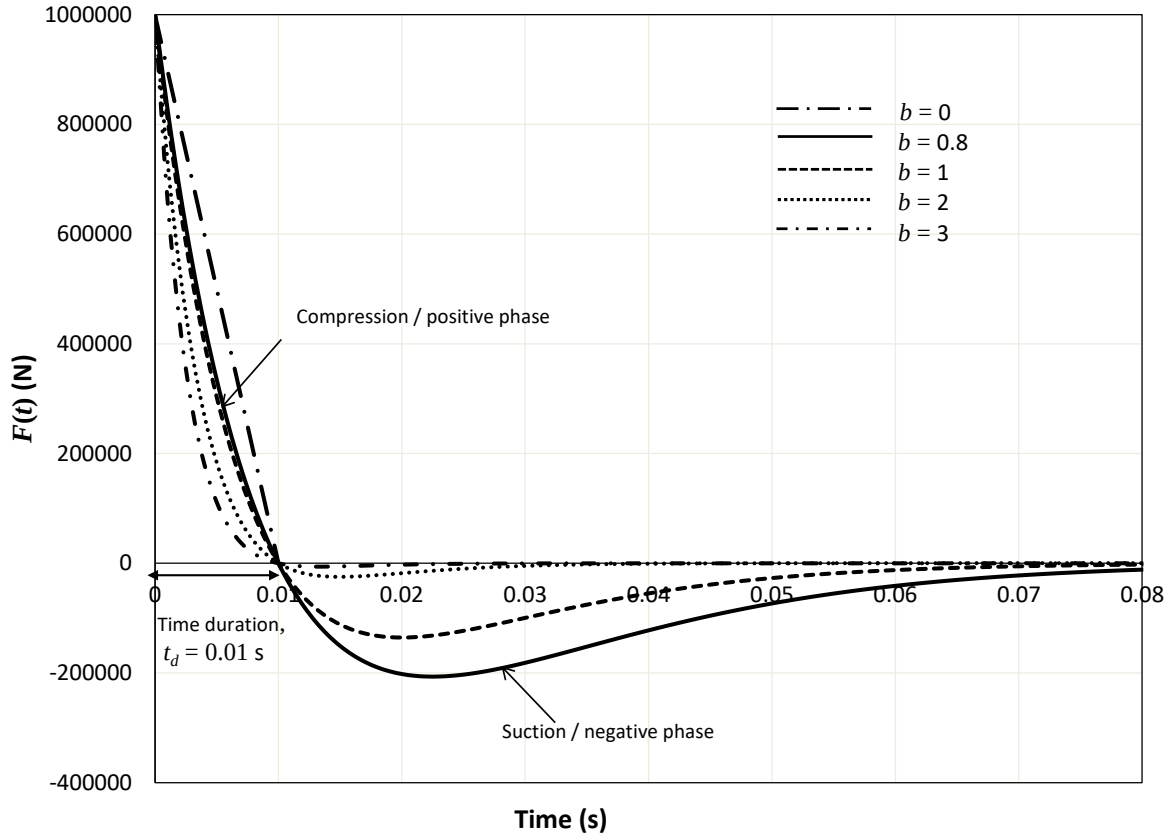

Fig. 1. Pulse loading variation with time for decay coefficients.

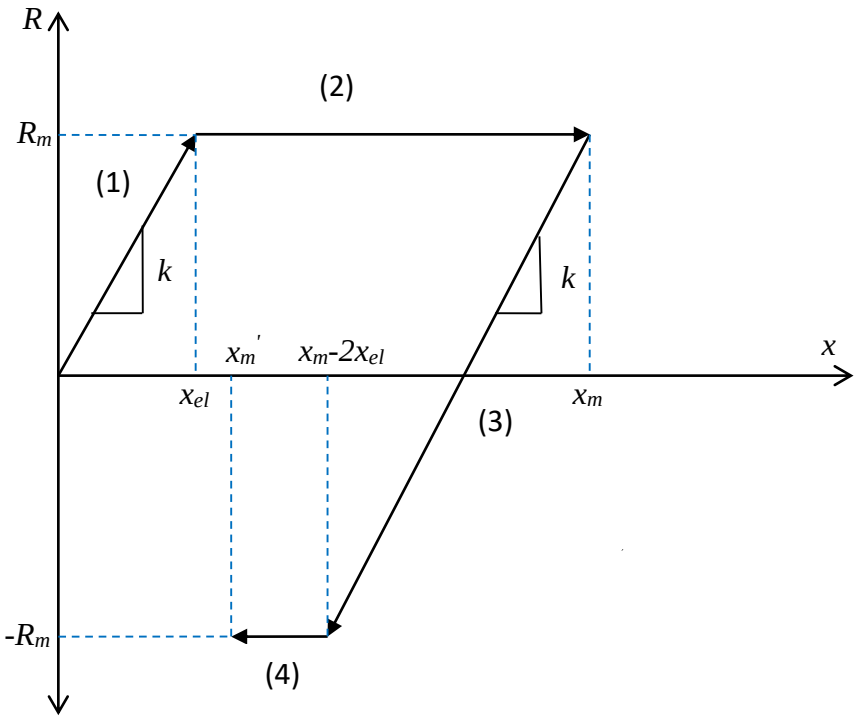

Fig. 2. Resistance-displacement relationship of an EPP-SDOF system.

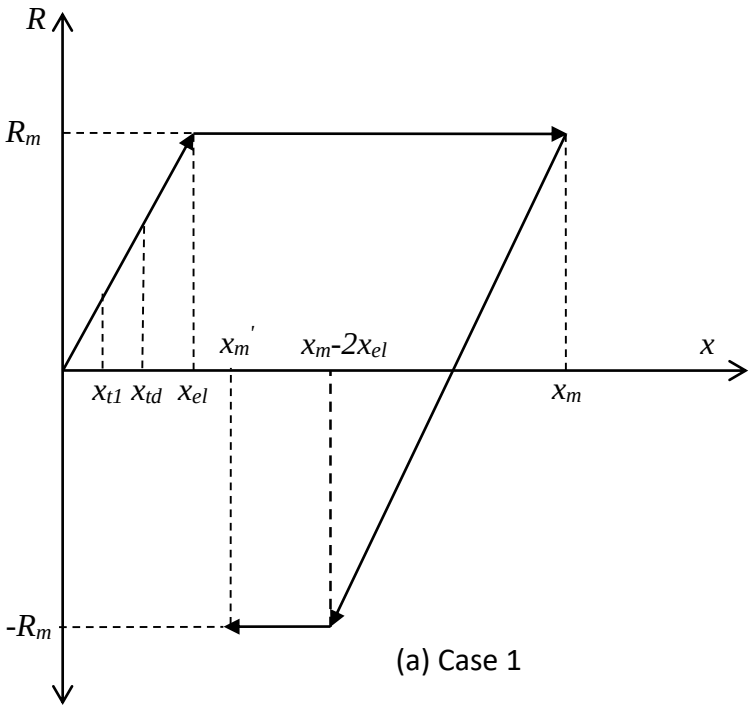

(a) Case 1

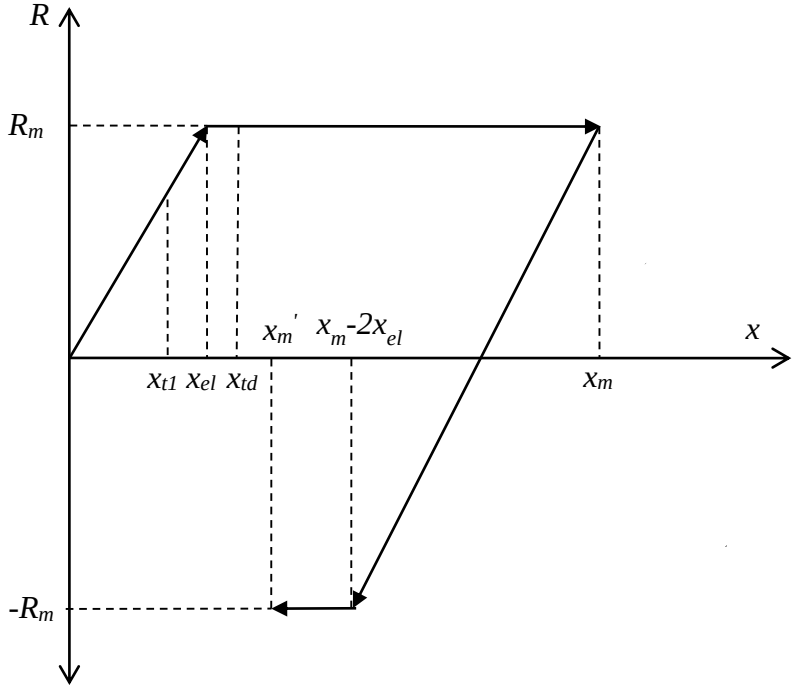

(b) Case 2

Fig. 3. Two cases of analysis

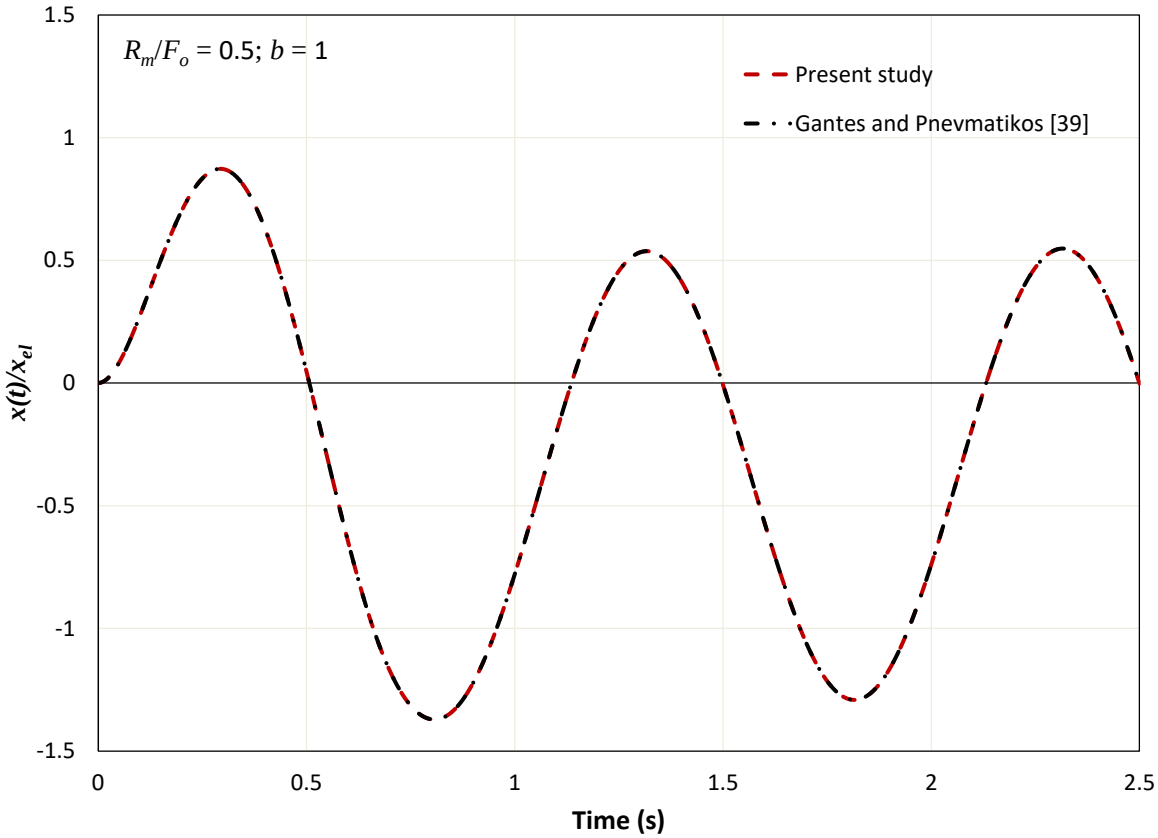

Fig. 4. Validation with work of Gantes and Pnevmatikos [39].

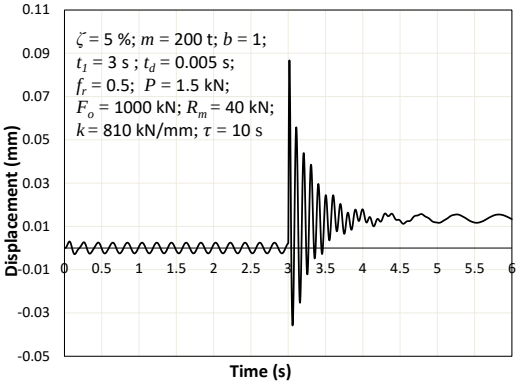

(a) τ = 10 s

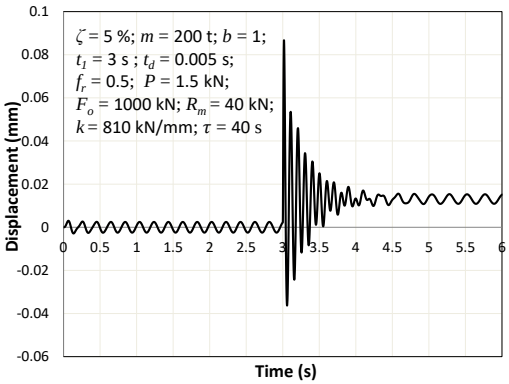

(b) τ = 40 s

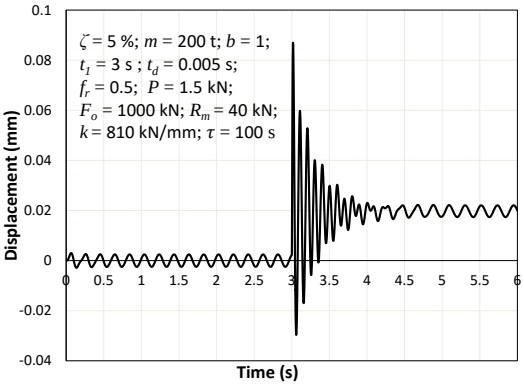

(c) τ = 100 s

Fig. 5. Response of the SDOF system to the various time constant values: Case 1.

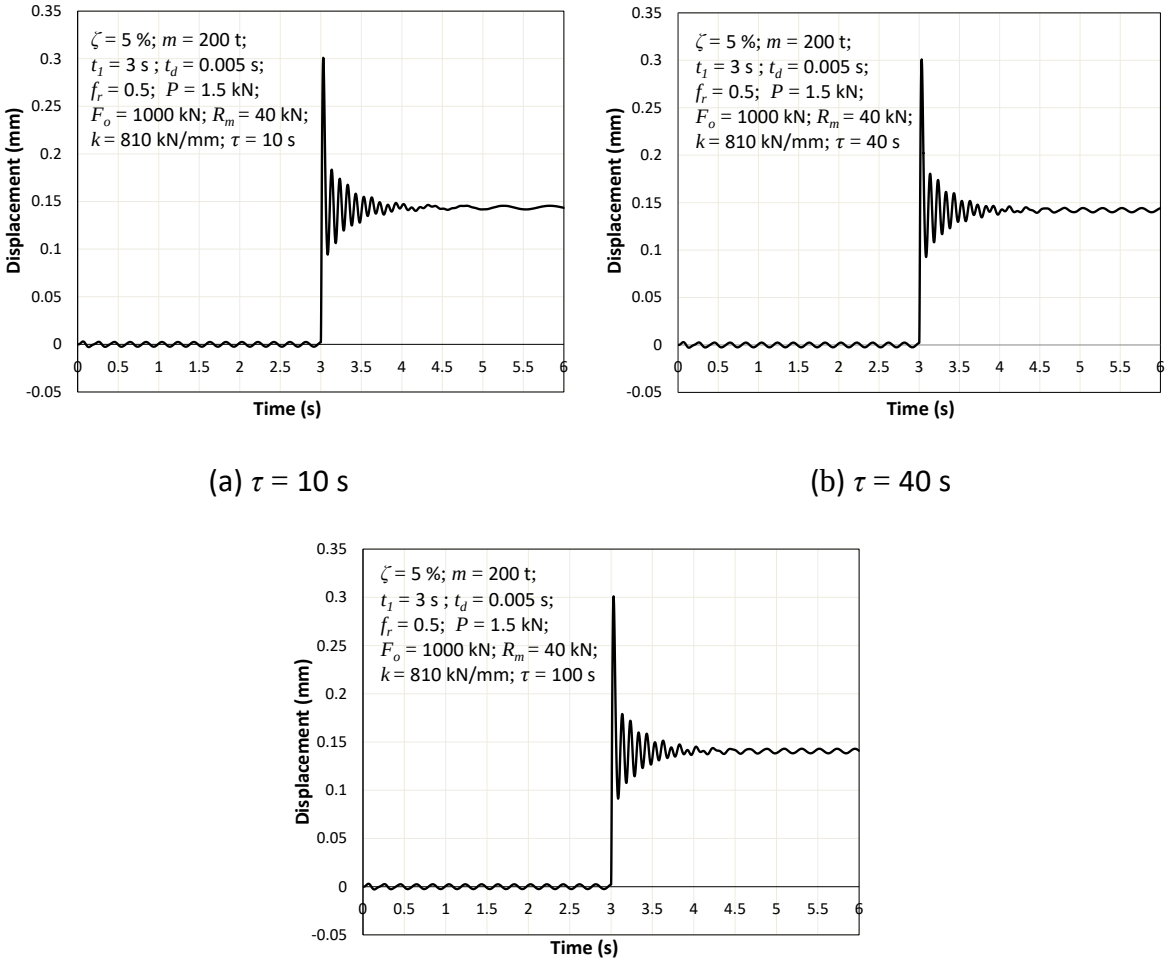

(a) τ = 10 s

(b) τ = 40 s

(c) τ = 100 s

Fig. 6. Response of the SDOF system to the various time constant values: Case 2.

Kirtika Samanta recently received her PhD in Geotechnical Engineering from Indian Institute of Technology Roorkee, India. She completed her Masters' degree from BIT Mesra, India. Her interest includes analytical and numerical modeling.

Priti Maheshwari received her PhD in Geotechnical Engineering from Indian Institute of Technology Kanpur, India. She is a Professor in Department of Civil Engineering of Indian Institute of Technology Roorkee, India. Her research areas include ground modeling and analysis, numerical methods in geomechanics, ground improvement, probabilistic analysis in geomechanics, and rock mechanics and rock engineering.

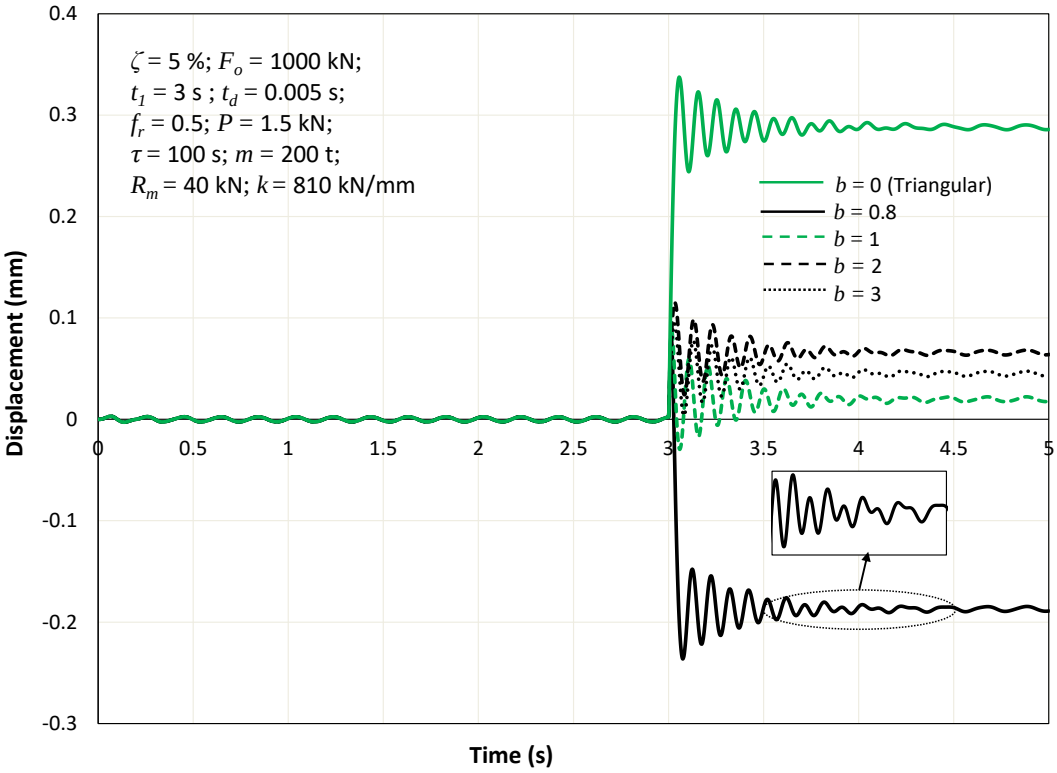

(a) Case 1

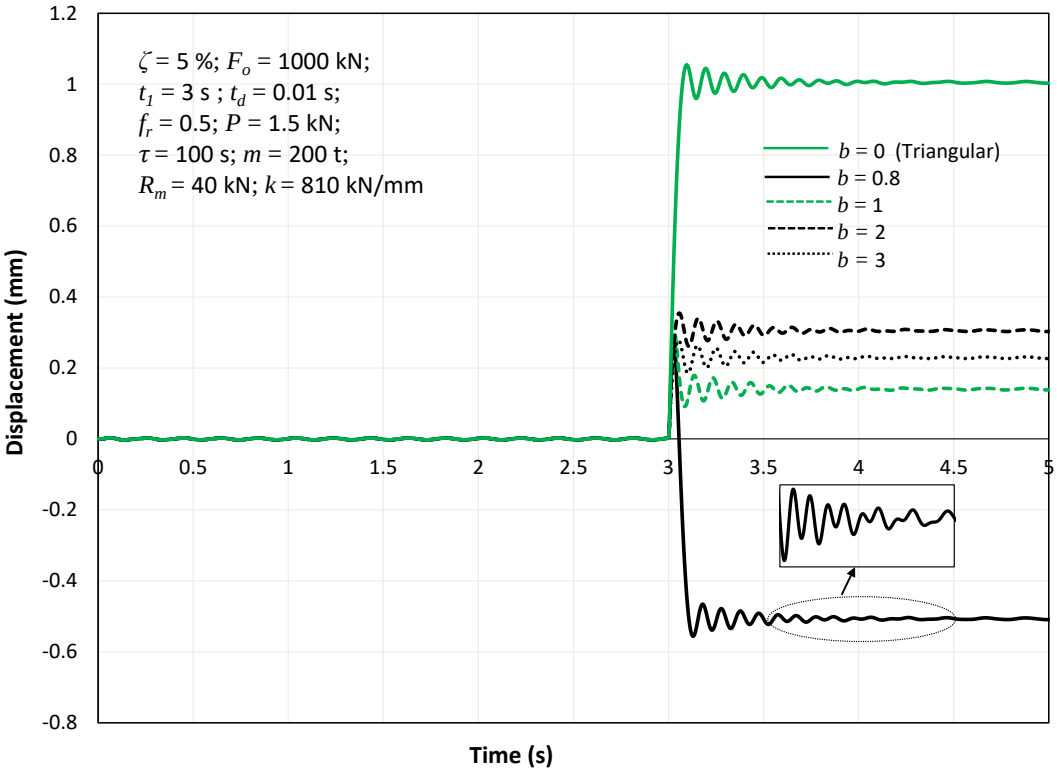

(b) Case 2

Fig. 7. Influence of decay coefficient on the response of the SDOF system.

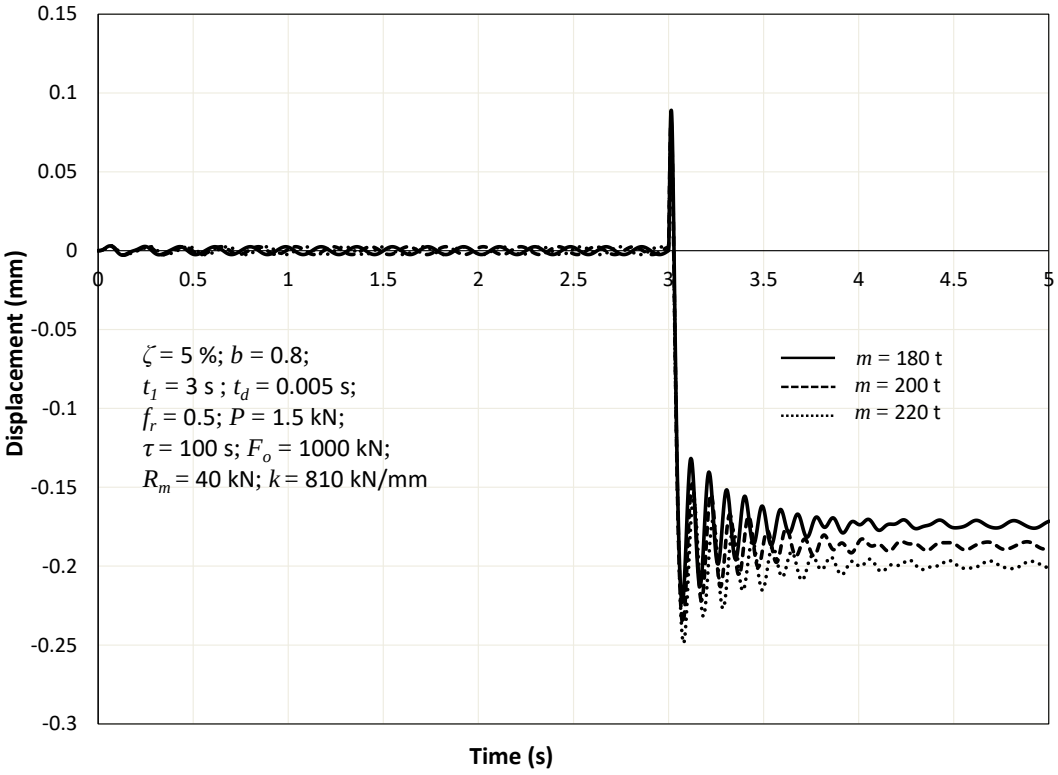

(a) Case 1

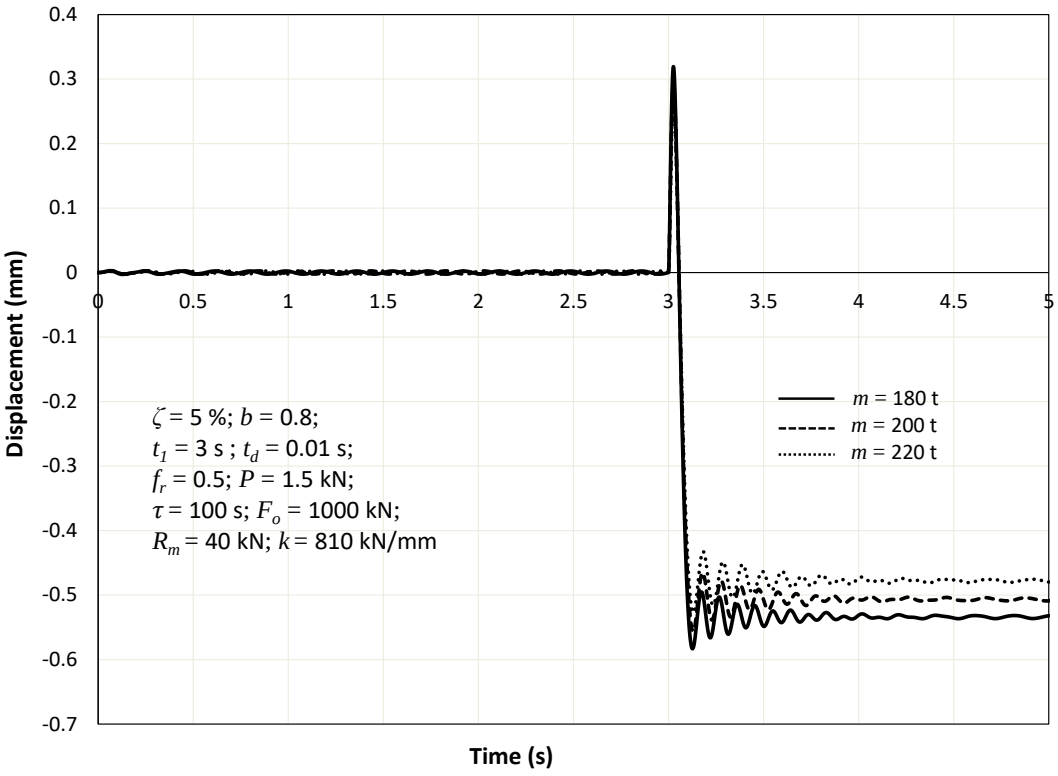

(b) Case 2

Fig. 8. Response of the SDOF system for variation in mass.

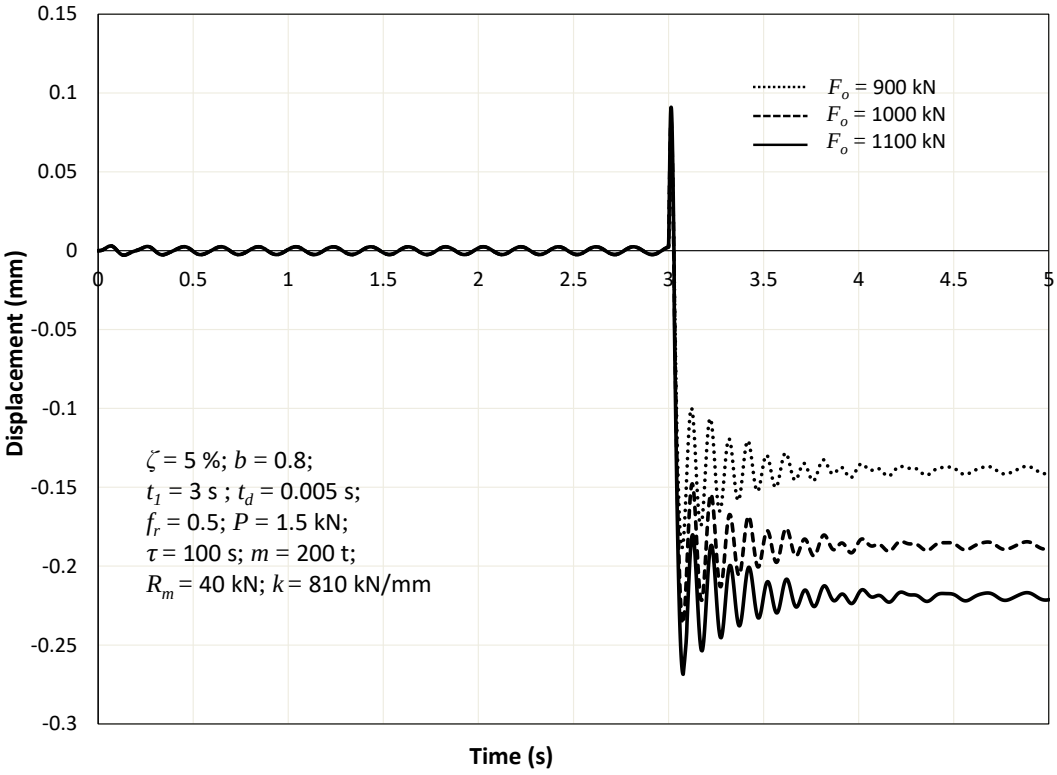

(a) Case 1

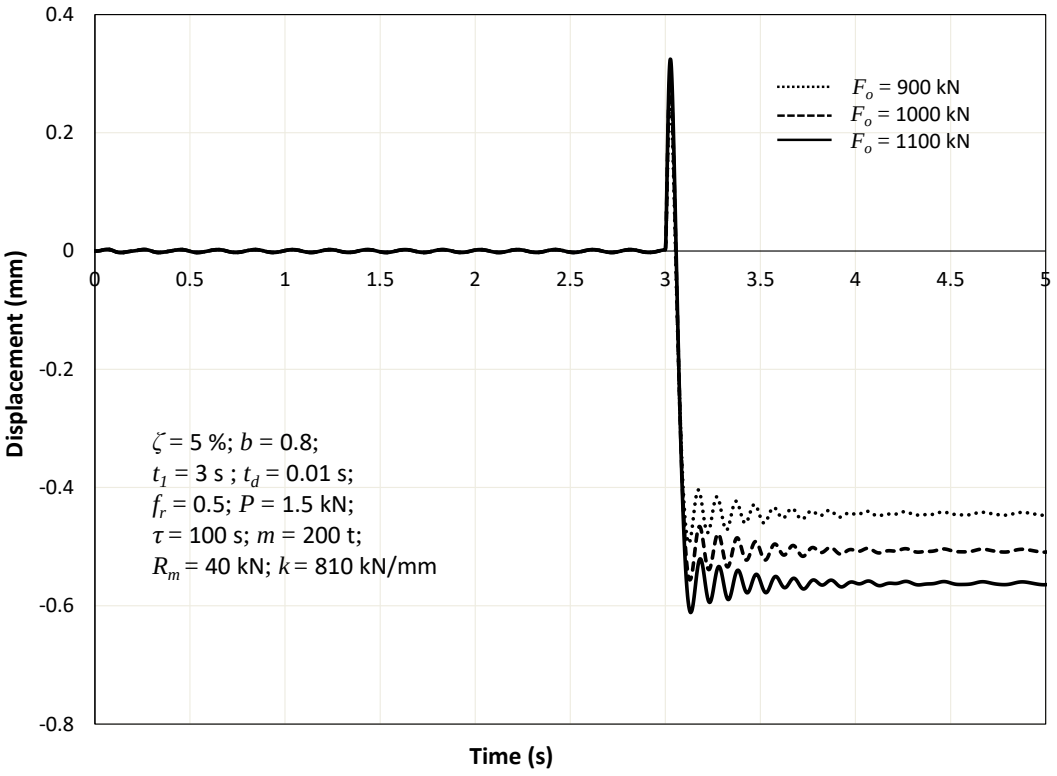

(b) Case 2

Fig. 9. Response of the SDOF system for variation in peak pulse magnitude

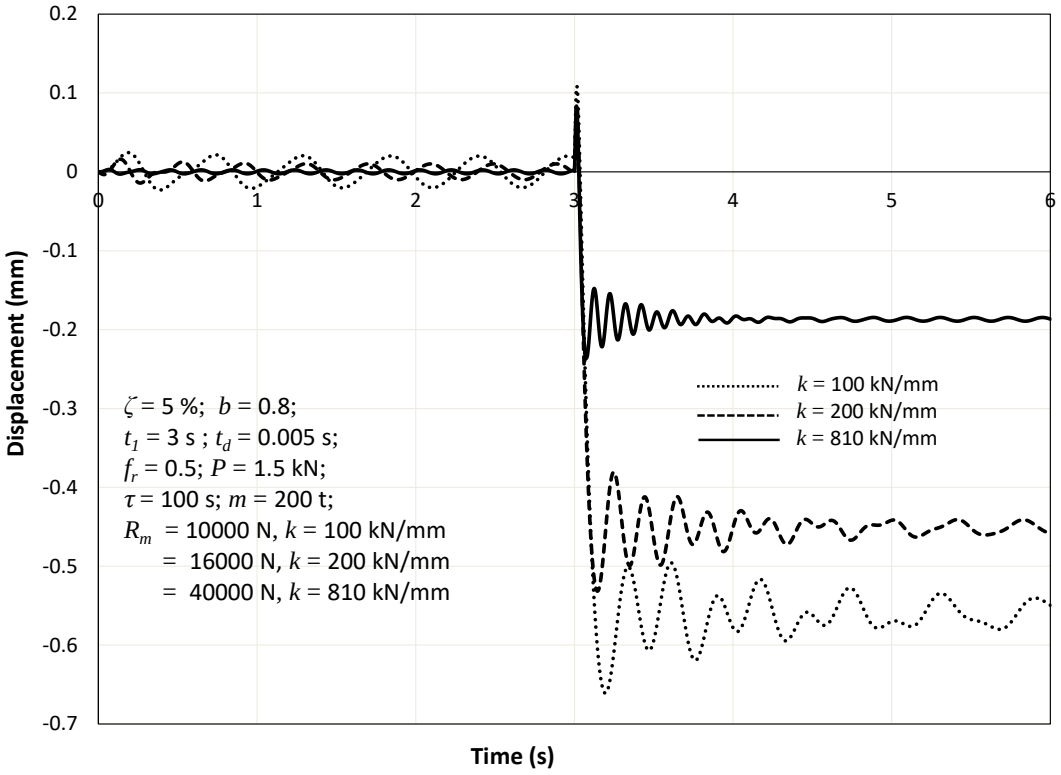

(a) Case 1

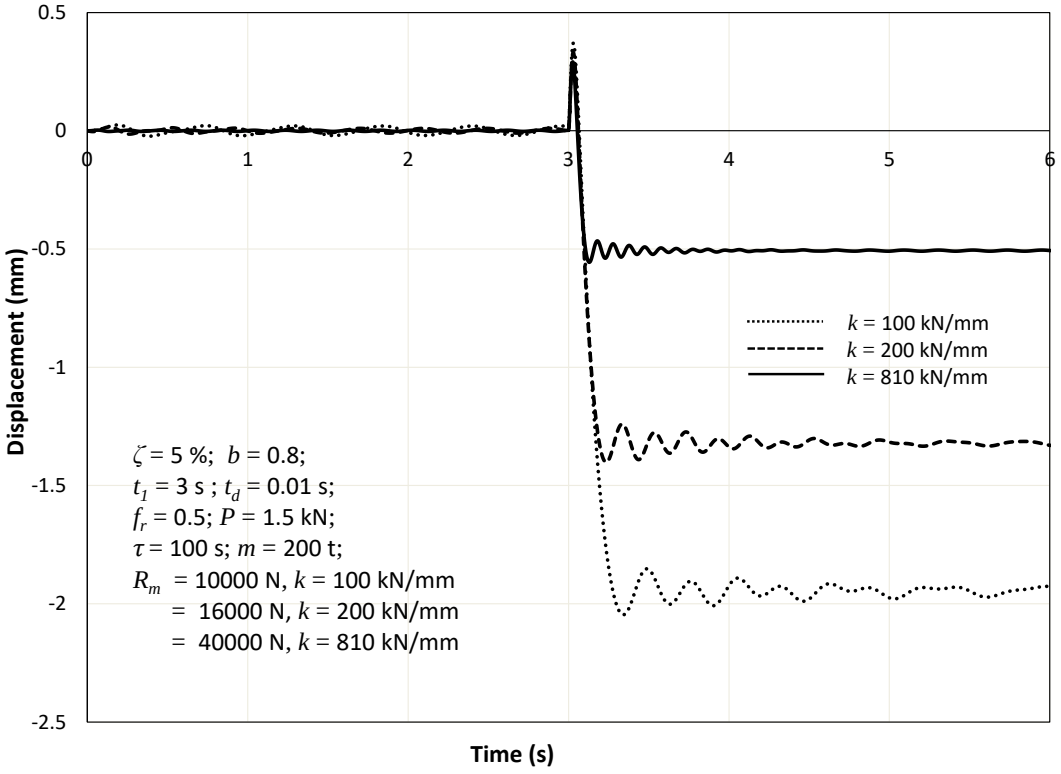

(b) Case 2

Fig. 10. Response of the SDOF system for different values of stiffness

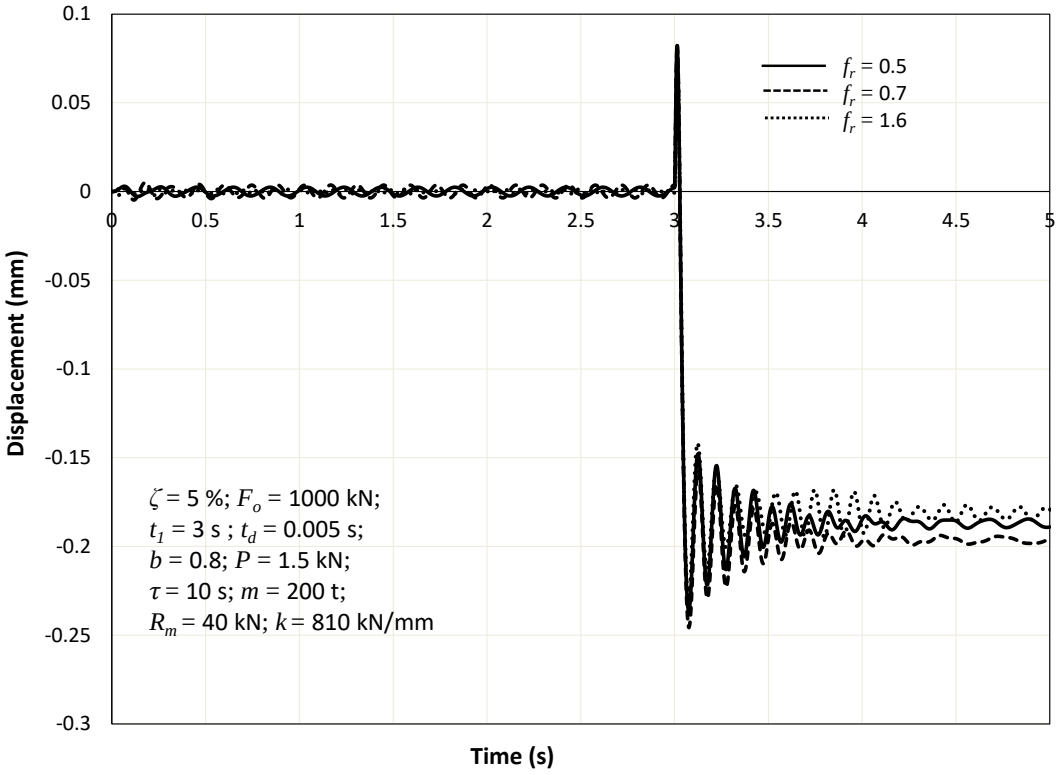

(a) Case 1

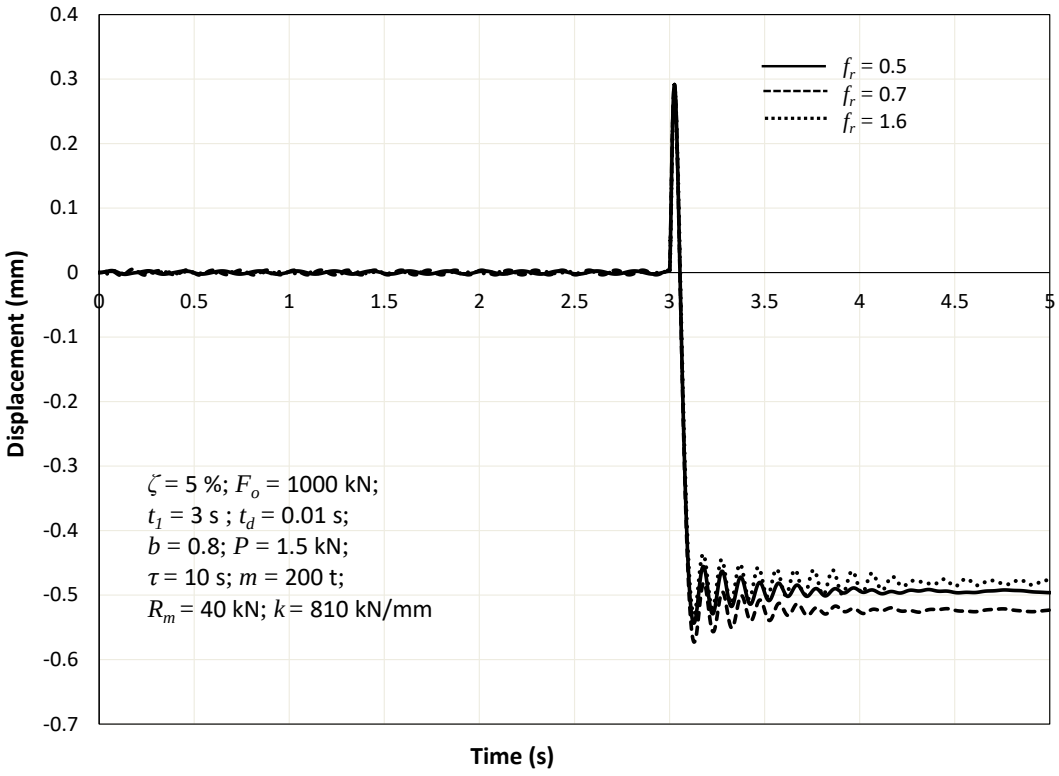

(b) Case 2

Fig. 11. Response of the SDOF system for different values of the frequency ratio.

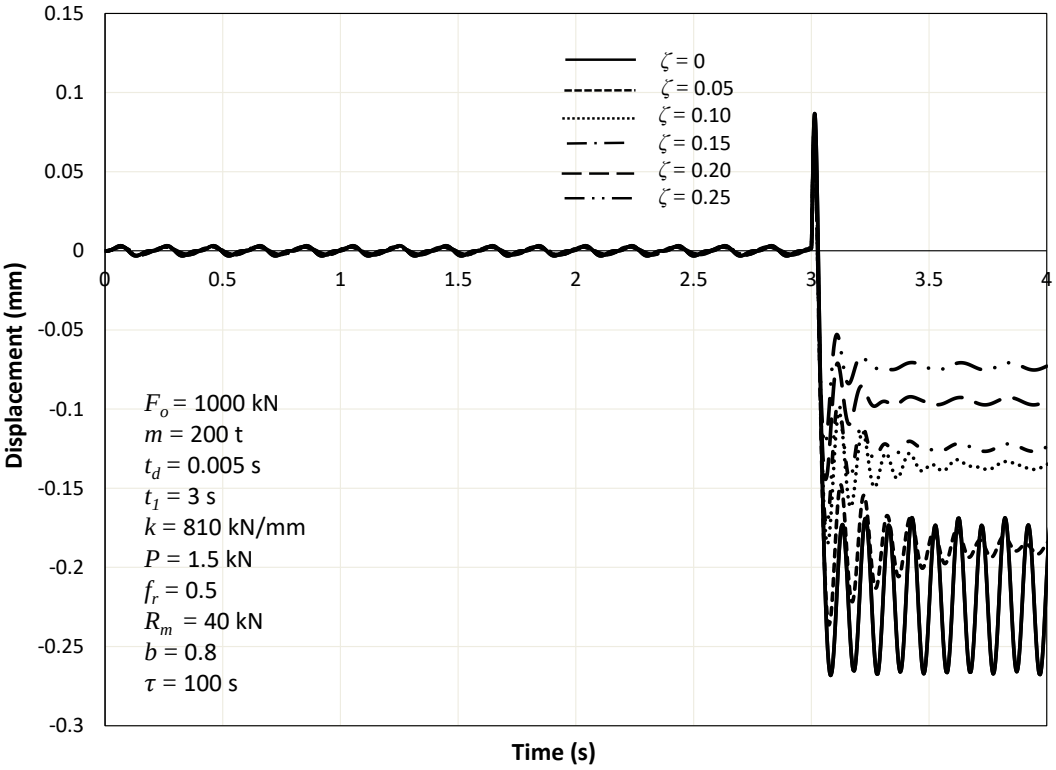

(a) Case 1

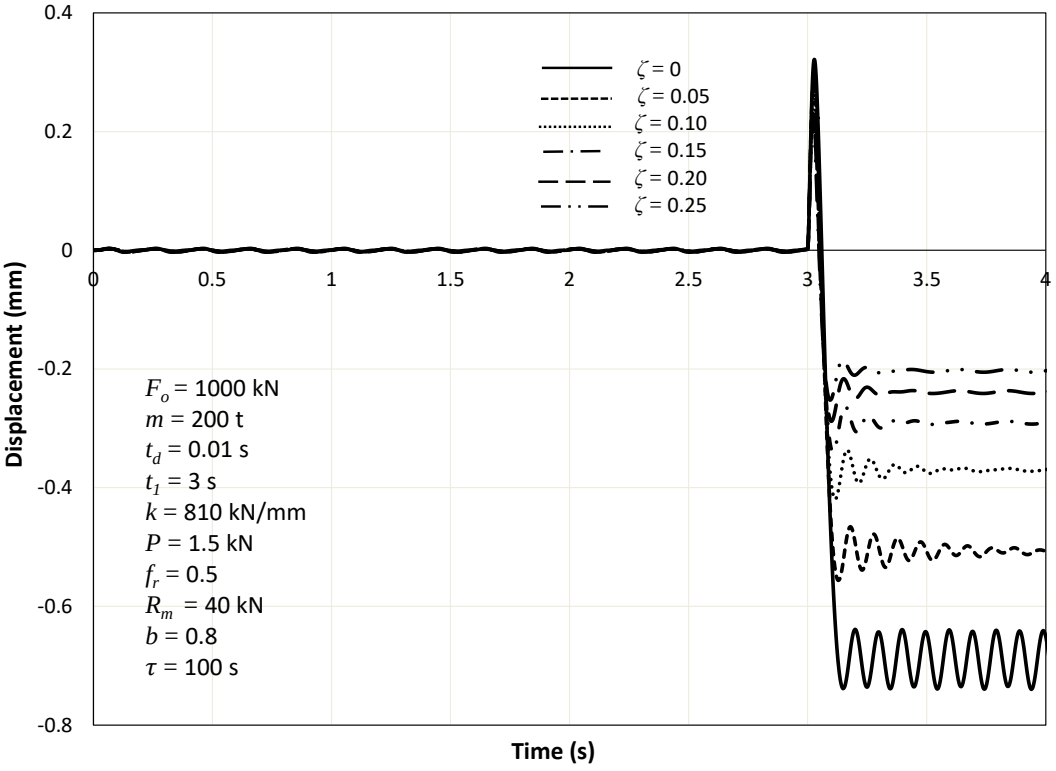

(b) Case 2

Fig. 12. Response of the SDOF system for different values of damping ratios.